Published in final edited form as:
Invest Ophthalmol Vis Sci. 2009 April ; 50(4): 1880–1885. doi:10.1167/iovs.08-2958.

Quantitative Mapping of Ion Channel Regulation by Visual Cycle Activity in Rodent Photoreceptors In Vivo

Bruce A. Berkowitz[1,2], **Robin Roberts**[1], **Deanna A. Oleske**[1], **Myungwon Chang**[1], **Stephen Schafer**[1], **David Bissig**[1], and **Marius Gradianu**[1]

1*Department of Anatomy and Cell Biology, Wayne State University, Detroit, Michigan*

2*Kresge Eye Institute, Wayne State University, Detroit, Michigan*

Abstract

Purpose—To test the hypothesis that the extent of outer retina uptake of manganese, measured noninvasively with manganese-enhanced MRI (MEMRI), is a quantitative biomarker of photoreceptor ion channel regulation by visual cycle activity.

Methods—Four groups of animals were studied: control rats adapted to three different background light intensities, darkadapted control mice systemically pretreated with retinylamine, and dark-adapted mice with a nonsense mutation in exon 3 of the *RPE65* gene (RPE65^{rd12}) with and without systemic 11-*cis*-retinal pretreatment. In all cases, rodents were anesthetized and studied with MEMRI 4 hours after manganese administration IP. Central retinal thickness and intraretinal ion channel regulation were measured from the MEMRI data.

Result—No differences ($P > 0.05$) in retinal thickness were noted within any arm of this study. In rats, manganese uptake was inversely proportional to the background light intensity in the outer retina but not in the inner retina. Specific inhibition at the level of RPE65 activity, either acutely with retinylamine or chronically in RPE65^{rd12} mice, similarly reduced ($P < 0.05$) outer retinal manganese uptake compared with that in control mice. In RPE65^{rd12} mice, outer retinal manganese uptake returned to normal ($P > 0.05$) after 11-*cis* retinal treatment. Inner retinal uptake was supernormal ($P < 0.05$) in retinylamine-treated mice but normal in untreated or 11-*cis* treated RPE65^{rd12} mice.

Conclusions—The present data support measuring the extent of manganese uptake in the outer retina as an analytic noninvasive metric of visual cycle regulation of photoreceptor ion channel activity in vivo.

Normal vision involves conversion of photons to electrical activity in the retina. In rod photoreceptors, this process starts when light interacts with rhodopsin (which consists of opsin and covalently bound 11-*cis*-retinal) to produce a *cis*-to-*trans* isomerization. Through a series of signal transduction steps, this isomerization causes cyclic guanosine monophosphate (cGMP)- gated ion channels in rods, which are maximally opened in the dark, to close in a graded fashion depending on the light intensity.[1,2] Rhodopsin and 11-*cis*-retinal are regenerated via the visual cycle to produce fresh rhodopsin. A key step in the visual cycle involves retinal pigment epithelium-specific protein 65 kDa (RPE65), an isomerase that converts all-*trans* retinol back to 11-*cis*-retinal.[3] Prolonged impairment of the visual cycle

Corresponding author: Bruce A. Berkowitz, Department of Anatomy and Cell Biology, Wayne State University School of Medicine, 540 E. Canfield, Detroit, MI 48201; E-mail: baberko@med.wayne.edu..

Disclosure: **B.A. Berkowitz**, None; **R. Roberts**, None; **D.A. Oleske**, None; **M. Chang**, None; **S. Schafer**, None; **D. Bissig**, None; **M. Gradianu**, None

resulting in inhibited 11-*cis*-retinal production—for example, by long-term inhibition of RPE65 activity—can produce persistent build-up of unbound opsin to concentrations high enough to induce chronic channel closure, which is linked with photoreceptor degeneration.[4] New pharmaceutical and gene therapies are being developed to address abnormal visual cycle activity and associated retinal degeneration. As these treatment options enter clinical trials, there is a need for noninvasive metrics of abnormal visual cycle activity in focal retinal regions (to identify which locations are most likely to benefit from treatment intervention before overt retinal thinning is evident), and, after different dosage schedules and concentrations of treatments for visual cycle abnormalities, can prognostically measure local rescue efficacy in emerging retinopathy.[5]

Currently, the electroretinogram (ERG) and optical coherence tomography (OCT) have been essential in documenting overall progression and treatment response for retinal dystrophy.[5] However, ERG and OCT measure neither regional changes in ion channel regulation via visual cycle activity nor the spatial relationship between ion channel activity and retinal thickness. To corroborate and extend ERG and OCT results, new methods are needed that can sensitively measure thickness and predystrophy changes in local visual cycle regulation of ion channel activity in vivo.

Manganese-enhanced MRI (MEMRI) is a noninvasive method that allows for simultaneous measurement of regional retinal uptake of manganese ion (Mn^{2+}, a strong MRI contrast agent and biomarker for regulation of ions such as calcium) colocalized with retinal thickness, after systemic injection of a modest and nontoxic amount of $MnCl_2$.[6-8] We have found that MEMRI is sensitive to the state of cGMP-gated channels, since significantly more manganese was taken up in the outer retina in dark-adapted rodents relative to that in light adapted rodents.[8] Although the evidence obtained thus far is suggestive of a relationship between visual cycle regulation of outer retinal ion activity and manganese uptake during physiologic adaptation, more work is needed to better define the quantitative nature of this relationship, to determine how it might be affected with visual cycle abnormalities, and to begin to establish its relevance in guiding therapeutic intervention for photoreceptor degeneration.

In this study we tested the hypothesis that the extent of outer retina uptake of manganese is a quantitative biomarker of photoreceptor ion channel regulation by visual cycle activity. At intermediate light intensities, photoreceptors respond to background light levels with a proportionate closure of the ion cation channels.[1] It is not yet known if such a graded response is reflected in the extent of outer retinal manganese uptake in rodents. We also examined the sensitivity of MEMRI to specific inhibition of the visual cycle at the level of RPE65 that subsequently reduces 11-*cis*-retinal production, which is expected to result in a buildup of unbound opsin and closure of photoreceptor ion channels.[4,9,10] MEMRI was used to study dark-adapted control mice and mice systemically pretreated with retinylamine.[9] A single application of retinylamine produces a long-lasting but impermanent inhibition of 11-*cis*-retinal production without associated retinal degeneration.[9] We chose to examine overnight dark-adapted animals to optimize detection sensitivity to conditions associated with either light or diseas-induced channel closure. In addition, we investigated, before degeneration was apparent, dark-adapted mice with a nonsense mutation in exon 3 of the *Rpe65* gene ($RPE65^{rd12}$) that effectively inhibits 11-*cis*-retinal production and results in retinal dystrophy by 7 months of age and $RPE65^{rd12}$ mice treated with systemic 11-*cis*-retinal.[10,11]

Methods

The animals were treated in accordance with the NIH Guide for the Care and Use of Laboratory Animals and the ARVO Statement for the Use of Animals in Ophthalmic and Vision Research. In all cases, rats or mice were housed and maintained in a normal 12 hour/12 hour light/dark

cycle. The day before the MRI experiment, rodents were placed and maintained in total darkness overnight. All procedures (e.g., weighing animals, injecting $MnCl_2$, anesthesia for MRI, and MRI examination) were performed in dim red light, darkness, or the light level being studied. $MnCl_2$ was administered as an intraperitoneal injection to awake rats (44 mg/kg) or mice (66 mg/kg), as described previously (Roberts R, et al. *IOVS* 2008;43:ARVO E-Abstract 4926).[7,8] Different doses were necessary, since, in a preliminary study, the 44-mg/kg dose of $MnCl_2$ did not produce reliable contrast changes in the mouse retina (data not shown), possibly due to the relatively higher overall metabolic rate in the mouse. Instead, it was found empirically that a somewhat higher dose of manganese (66 mg/kg) produced more robust retinal contrast changes. In all cases, rodents were maintained awake in dark conditions for another 3.5 hours, anesthetized, and imaged (MEMRI study).

Experimental Arms

Light/Dark—Male albino control Sprague-Dawley (SD) rats (204-276 g; mean age, 46 days) were examined with MEMRI after exposure to the following light intensities: 1.8 ± 0.7 (n = 10, mean ± SEM), 51.3 ± 11.7 (n = 5), and 250.2 ± 19.3 (n = 6) lux. Light meter (traceable dual-range light meter; Control Co., Friendswood, TX) values were multiplied by 0.91 to correct fluorescent light values to the tungsten light calibration values. The intermediate light levels were produced by positioning the cage different distances from a 25-W fluorescent light bulb. Every hour after manganese administration, intensity readings were obtained at the brightest and dimmest portions of the cage and averaged; mean readings over the 4-hour time course (before the MEMRI experiment) were then averaged.

Retinylamine—Two groups were studied in this arm of the study: noninjected C57BL/6 mice (n = 8 males; 28-33 g; mean age, 184 days) and C57BL/6 mice (n = 6 males; 27-32 g; mean age, 184 days) treated with retinylamine (kind gift of Martin Golczak and Krzysztof Palczewski, Case Western Reserve University, Cleveland, OH).[9] For each treated mouse, retinylamine (0.5 mg) was dissolved in DMSO (100 μL) and injected intraperitoneally. The next day, treated mice were briefly anesthetized with ether. Their eyes were dilated with 1 drop of atropine and they were allowed to fully wake up. They were then positioned close to laboratory lights (300 lux) for 4 hours to ensure the remaining rhodopsin levels were bleached. In all cases, the mice were dark adapted overnight, during the injection, and MEMRI examination. These two groups had similar extraocular muscle signal intensities (as reported in the results section) implying similar whole body handling of manganese (i.e., no DMSO effect).

RPE65^{rd12}—In this arm of the study, the following groups were examined with MEMRI: noninjected C57BL/6 mice (n = 4 males; 26-29 g; mean age, 90 days) and noninjected RPE65^{rd12} on a C57BL/6 background (n = 4 males; 16-20 g; mean age, 35 days; Jackson Laboratories, Bar Harbor, ME).[10] In addition, 11-*cis*-retinal (approximately 188 μg/mouse, obtained through an NEI program (http://www.nei.nih.gov/funding/11_cis_retinal.asp) was constituted in ethanol and bovine serum albumin and administered as a 0.7 mL bolus IP to RPE65^{rd12} mice (n = 3 males; 17-20 g; mean age, 42 days; Jackson Laboratories).[11] Note that the 11-*cis*-retinal formulation and administration used in this study killed three other RPE65^{rd12} mice and impaired systemic handling of manganese in three surviving RPE65^{rd12} mice that required correction (*vide infra*). In all cases, the mice were dark adapted overnight, during the injection, and during the MEMRI examination. Note that C57BL/6 mice have the methionine amino acid at codon 450 of the *RPE65* gene.[12]

Manganese-Enhanced MRI—Immediately before the MRI experiment, each animal was anesthetized with urethane (36% solution, IP 0.083 mL/20 g animal weight, prepared fresh daily; Aldrich, Milwaukee, WI). In addition, some mice received an injection of xylazine (1-8

mg/kg, IP). In mice, urethane was found to increase respiratory frequency and thus motion artifacts on MEMRI. The addition of a small amount of the muscle relaxant xylazine helped to minimize these artifacts. To maintain the core temperature, a recirculating heated water blanket was used. Rectal temperatures were continuously monitored throughout each experiment, as previously described.[13] MRI data were acquired on a 4.7-T system (Avance; Bruker AXS, Madison, WI) using a two-turn transmit/receive surface coil (1.0 cm diameter) placed over the eye. Images were acquired with an adiabatic spin-echo imaging sequence (repetition time [TR], 350 seconds; echo time [TE], 16.7 ms; number of acquisitions [NA], 16; matrix size, 512 × 512; slice thickness, 620 μm; field of view, 12 × 12 mm^2; 54 minutes/image).[14] A single transverse slice through the center of the eye (based on sagittal localizer images collected using the same adiabatic pulse sequence as just described) was obtained for each animal.

Data Analysis

Retinal Thickness—Whole retinal thicknesses were determined from each MEMRI-generated image as the radial distance between the anterior edge and the posterior edge of the retina at distances ± 0.4 to 1 mm from the optic nerve.[15] Briefly, in-house written software was used to map the in situ image into a linear representation for each retina. Thicknesses were derived from these linearized images. First, the average signal intensity profile as a function of depth into the retina was determined by the program. Then, the point at which the signal intensity profile crosses the average of the highest and lowest signal intensity at the provisional vitreous/retina and retina/choroid+sclera boundaries was calculated automatically. The distance between these two midpoints was considered the whole retinal thickness. We confirmed a difference of less than 10 μm between the automatically derived whole retinal thicknesses and those thicknesses derived manually from the same retina (data not shown). In animals with a light-adapted manganese uptake pattern, inner retinal thicknesses were similarly derived. Mean superior and inferior values generated for each animal group were averaged and used for comparisons.

Layer-Specific Signal Intensity—Within each group, individual linearized retinas were averaged into a composite image and used for visual comparison purposes only.

For quantitative analysis, signal intensities were analyzed using the program NIH IMAGE (developed by Wayne Rasband, National Institutes of Health, Bethesda, MD; available at http://rsb.info.nih.gov/ij/index.html) and derived macros.[16] Changes in receiver gain between animals were controlled for by setting the signal intensity of a fixed region of noise in each image to a fixed value. In all retinas, a 1-pixel-thick line (representing the border between inner and outer retina) was set at 4 pixels (or approximately 94 μm) posterior to the clearly defined vitreoretinal division. Another 1-pixel-thick line was set at 3 pixels (or approximately 70 μm) posterior to this inner/outer division. Pixels immediately anterior to each line were considered representative of the inner and outer retina, respectively, and were analyzed as previously described.[8] These retinal regions are also indicated in Figure 2.

Extraocular muscle signal intensities for each animal were measured from a fixed-size ellipse-shaped region-of-interest drawn in the anterior-most aspect of the inferior rectus muscle. Animals that did not have a recognizable rectus muscle due to head and slice orientation were not included in the extraocular muscle analysis.

Statistical Analysis

The retinal thicknesses were consistent with a normal distribution, and comparisons between groups were performed by unpaired two-tailed *t*-test. Comparison of retinal signal intensities and Mn^{2+} ion enhancements were performed in a generalized estimating equation approach.

[8] By this method, we performed a general linear regression analysis using all the pixels from each subject and accounts for the within-subject correlation between adjacent pixels. In all cases, unless otherwise noted, a two-tailed $P < 0.05$ was considered significant.

Results

Background Light Intensity

In the rats, no significant differences in whole retinal thickness were detected ($P > 0.05$) between any of the groups (range, 195-213 μm) in this arm of the study. Figure 1 summarizes the effect of background light intensity adaptation on intraretinal manganese uptake. A inverse linear relationship was found for outer retinal uptake ($r = -0.99$, signal intensity = 90.9 - 3.84 [log10(light intensity)]); the slope was less than 0 ($P = 0.034$). In contrast, for inner retinal uptake, the slope was not different from 0 ($P = 0.38$).

Retinylamine

Untreated and treated mice had similar ($P > 0.05$) whole retinal thickness values (range, 213-218 μm). Visual inspection of mean linearized images of retina about the optic nerve suggested that pharmacologic inhibition at the level of RPE65 reduced outer retinal manganese uptake relative to that in untreated mice (Fig. 2A). Quantitative analysis supported a subnormal outer retinal uptake ($P < 0.05$; Figs. 2B, 2C). In addition, inner retinal uptake was supernormal ($P < 0.05$) in retinylamine-treated mice. Extraocular muscle intensity of the control (72.3 + 6.4 AU, $n = 6$) and retinylamine (88.9 ± 4.4 AU, $n = 6$) groups were not different ($P > 0.05$).

RPE65^{rd12} Mice

The whole retinal thickness of the similarly aged WT control, untreated RPE65^{rd12}, and treated RPE65^{rd12} mice were not significantly different from each other (range, 198-201 μm). The inner retinal manganese uptake of dark-adapted control and RPE65^{rd12} mice were not different ($P > 0.05$). Outer retinal uptake of dark-adapted RPE65^{rd12} mice was reduced ($P < 0.05$) to that expected for light adaptation. On the whole body level, these two groups appeared to handle manganese similarly, since extraocular muscle intensity of these control (90.2 ± 2.4 AU, $n = 7$) and RPE65^{rd12} (84.6 ± 6.3 AU, $n = 4$) were not different ($P > 0.05$).

After systemic administration of 11-*cis*-retinal to the RPE65^{rd12} mice, subnormal uptake of manganese in inner and outer retina was noted (data not shown). In these animals, extraocular muscle signal intensities were also reduced (74.3 ± 6.8 AU, $n = 3$) relative to WT control values ($P \leq 0.06$), suggesting that the injection solution reduced systemic manganese transport and uptake, perhaps due to the relatively high ethanol content and not to the 11-*cis*-retinal, per se. To compensate, an inner retina-specific scaling factor of 1.24 was used to bring inner retinal values in line with the WT control values. This scaling factor was also applied to the outer retinal values. After this procedure, outer retinal uptake in treated dark-adapted RPE65^{rd12} mice was not different from WT control values ($P > 0.05$) but was different ($P < 0.05$) from that of untreated RPE65^{rd12} mice (Fig. 3).

Discussion

The data in this study support our hypothesis that the extent of outer retina uptake of manganese is a quantitative biomarker of photoreceptor ion channel regulation by visual cycle activity. First, in rats, the extent of outer retinal uptake of manganese was linearly inversely proportional to the log of light intensity used for adaptation. This relationship mirrored that reported between background light adaptation and extracellular current in isolated rod photoreceptors.[1] Our use of fluorescent light and inability to directly measure the exact light intensity striking the retina complicates closer comparisons with the literature. Nonetheless, the MEMRI studies set the

stage for future work which may bridge the gap between in vitro and in vivo studies by measuring retinal manganese uptake response to, for example, different background monochromatic light adaptation.

Second, in dark-adapted mice, acute or chronic inhibition of the visual cycle at the level of RPE65 decreased the amount of manganese taken up in the outer retina relative to that in dark-adapted mice without such visual cycle manipulation. RPE65 is a pathogenic visual cycle target associated with the retinal degenerative disease Leber congenital amaurosis.[17] Thus, these data underscore the sensitivity of MEMRI to inhibition of the visual cycle with relevance to human disease. Of note, a similar degree of manganese uptake in the outer retina was found for both fully light adapted rats (Fig. 1B) and dark-adapted mice with pharmacologic (Fig. 2C) or genetically induced RPE65 (Fig. 3) abnormalities. This result may reflect the fact that the photoreceptor layer of rats and mice are similarly rod dominated.[18,19]

Third, in dark-adapted $RPE65^{RD12}$ mice, systemic 11-*cis*-retinal administration corrected the level of manganese uptake in outer retina to dark-adapted values, after adjusting for systemic effects of the injection. This adjustment, derived only from inner retinal intensities and then applied to outer retina values, appears reasonable given our assessment of impairment in how the mice handled systemically injected manganese, based on a subnormal extraocular muscle signal intensity and lack of expected effect on inner retinal ion regulation after 11-*cis*-retinal administration. The present results are also consistent with data showing that systemically administered 11-*cis*- retinal improves rod function in RPE65 knockout mice.[11] To the best of our knowledge, 11-*cis*-retinal rescue has not been reported in the $RPE65^{RD12}$ mouse. Our data raise the possibility of using MEMRI to guide therapeutic intervention for photoreceptor degeneration associated with, but perhaps not limited to, visual cycle defects.

The relatively modest $MnCl_2$ doses (44 mg/kg [rats] to 66 mg/kg [mice]) used in the current study were not expected to adversely affect retinal anatomy and function, particularly in the few hours between injection and examination.[7,8] The somewhat higher dose used in mice, relative to that administered to rats in this study, was similar to, or lower than, that used in other mouse MEMRI studies, and is well below that needed to induce neurotoxicity.[20,21] Furthermore, as discussed earlier, the three major findings in this study are in line with established physiology and provide indirect evidence of a lack of manganese toxicity at the level of the visual cycle. These considerations support the 44 to 66 mg/kg dose range as nontoxic and intraretinal uptake of manganese as a quantitative biomarker of photoreceptor ion regulation by visual cycle activity in vivo.

MEMRI-derived retinal thicknesses in rat and mouse models is an accurate measure relative to standard histology.[7,8,22] The whole retinal thicknesses measured in this study are in agreement with these validated values. Note that in the present study the statistical thickness differences between groups were relatively subtle compared with the spatial resolution of the present MEMRI experiment and so some caution is needed to avoid overinterpretation of these data. Nonetheless, the similar thicknesses between experimental and respective control groups in each arm of the study were consistent with the expected lack of retinal edema (potentially due, for example, to manganese toxicity) or retinal thinning.

Our present hypothesis was motivated by data in a previous study in Royal College of Surgeons (RCS) rats in which the extent of intraretinal manganese uptake was disease-duration dependant.[6] We focused on changes in RCS intraretinal ion channel regulation that occur before overt dystrophy (at postnatal day [P]17) before the effects of retinal remodeling on ion channel regulation were altered in a potentially complicated and disease-specific manner. At P17, inner retinal manganese uptake in RCS rats was subnormal.[6] In contrast, with the manipulations of visual cycle activity in the present study, no decrease in inner retina uptake

was found. A possible explanation for this difference may involve the integrity of the ON and OFF pathways of the inner retina. RCS rats are reported to have inner retinal abnormalities, including channel defects and selective loss of ON pathway cells, early in the time course of the disease.[23,24] A roughly equal representation of ON and OFF cells is expected in the mice acutely treated with retinylamine and in the young RPE65^{RD12} mice examined in this study.[25] Of interest, acute inhibition of RPE65 with retinylamine was associated with supernormal uptake of manganese in the inner retina. It is possible that this was a temporary reactive response to inhibition of outer retinal processing, similar to that reported after acute sodium iodate exposure.[7] More work is needed to better understand the temporal evolution of this supernormal response after retinylamine injection as well as the underlying mechanism.

At P17, the outer retina of RCS rats appeared light adapted even after overnight dark adaptation.[6] In the RCS rat, a predegenerative visual cycle abnormality, subnormal rhodopsin dephosphorylation kinetics, has been reported.[26] We speculated that this abnormality could lead to suppressed cGMP-gated ion channel opening that, in turn, could explain the observed lower manganese entry into the outer retina.[4] The data in the present study support both this interpretation and measuring the extent of outer retina uptake of manganese with MEMRI as a quantitative biomarker of photoreceptor ion channel regulation by visual cycle activity.

In summary, measuring the degree of manganese uptake in the outer retina appears useful as an objective noninvasive metric of visual cycle regulation of photoreceptor ion channel activity in vivo. Our data clearly demonstrate channel closure in two models in which 11-*cis*-retinal production is inhibited and thus appears to provide first-time in vivo evidence supporting the presence of unbound opsin buildup in these models.

Acknowledgments

Supported by National Institutes of Health (NIH) Grant EY018109, NIH Mouse Metabolic and Phenotyping Centers Pilot and Feasibility Program, the Juvenile Diabetes Research Foundation, and an unrestricted grant from Research to Prevent Blindness.

References

1. Matthews HR, Fain GL. The effect of light on outer segment calcium in salamander rods. J Physiol 2003;552(3):763–776. [PubMed: 12949220]
2. Yau KW. Phototransduction mechanism in retinal rods and cones. The Friedenwald Lecture. Invest Ophthalmol Vis Sci 1994;35(1):9–32. [PubMed: 7507907]
3. Marlhens F, Bareil C, Griffoin JM, et al. Mutations in RPE65 cause Leber's congenital amaurosis. Nat Genet 1997;17(2):139–141. [PubMed: 9326927]
4. Fain GL. Why photoreceptors die (and why they don't). Bioessays 2006;28(4):344–354. [PubMed: 16547945]
5. Roman AJ, Boye SL, Aleman TS, et al. Electroretinographic analyses of Rpe65-mutant rd12 mice: developing an in vivo bioassay for human gene therapy trials of Leber congenital amaurosis. Mol Vis 2007;13:1701–1710. [PubMed: 17960108]
6. Berkowitz BA, Gradianu M, Schafer S, et al. Ionic dysregulatory phenotyping of pathologic retinal thinning with manganese-en-hanced MRI. Invest Ophthalmol Vis Sci 2008;49(7):3178–3184. [PubMed: 18362105]
7. Berkowitz BA, Roberts R, Luan H, et al. Manganese-enhanced MRI studies of alterations of intraretinal ion demand in models of ocular injury. Invest Ophthalmol Vis Sci 2007;48(8):3796–3804. [PubMed: 17652754]
8. Berkowitz BA, Roberts R, Goebel DJ, Luan H. Noninvasive and simultaneous imaging of layer-specific retinal functional adaptation by manganese-enhanced MRI. Invest Ophthalmol Vis Sci 2006;47(6): 2668–2674. [PubMed: 16723485]

9. Golczak M, Kuksa V, Maeda T, Moise AR, Palczewski K. Positively charged retinoids are potent and selective inhibitors of the transcis isomerization in the retinoid (visual) cycle. Proc Natl Acad Sci U S A 2005;102(23):8162–8167. [PubMed: 15917330]
10. Pang JJ, Chang B, Hawes NL, et al. Retinal degeneration 12 (rd12): a new, spontaneously arising mouse model for human Leber congenital amaurosis (LCA). Mol Vis 2005;11:152–162. [PubMed: 15765048]
11. Ablonczy Z, Crouch RK, Goletz PW, et al. 11-cis-Retinal reduces constitutive opsin phosphorylation and improves quantum catch in retinoid-deficient mouse rod photoreceptors. J Biol Chem 2002;277 (43):40491–40498. [PubMed: 12176991]
12. Nusinowitz S, Nguyen L, Radu R, Kashani Z, Farber D, Danciger M. Electroretinographic evidence for altered phototransduction gain and slowed recovery from photobleaches in albino mice with a MET450 variant in RPE65. Exp Eye Res 2003;77(5):627–638. [PubMed: 14550405]
13. Berkowitz BA, Ito Y, Kern TS, McDonald C, Hawkins R. Correction of Early subnormal superior hemiretinal deltaPO(2) predicts ther-apeutic efficacy in experimental diabetic retinopathy. Invest Ophthalmol Vis Sci 2001;42(12):2964–2969. [PubMed: 11687543]
14. Schupp DG, Merkle H, Ellermann JM, Ke Y, Garwood M. Localized detection of glioma glycolysis using edited 1H MRS. Magn Reson Med 1993;30(1):18–27. [PubMed: 8371670]
15. Cheng H, Nair G, Walker TA, et al. Structural and functional MRI reveals multiple retinal layers. Proc Natl Acad Sci U S A 2006;103(46):17525–17530. [PubMed: 17088544]
16. Berkowitz BA. Adult and newborn rat inner retinal oxygenation during carbogen and 100% oxygen breathing: comparison using magnetic resonance imaging delta Po2 mapping. Invest Ophthalmol Vis Sci 1996;37(10):2089–2098. [PubMed: 8814148]
17. den Hollander AI, Roepman R, Koenekoop RK, Cremers FPM. Leber congenital amaurosis: genes, proteins and disease mechanisms. Prog Retin Eye Res 2008;27(4):391–419. [PubMed: 18632300]
18. Carter-Dawson LD, Lavail MM, Sidman RL. Differential effect of the rd mutation on rods and cones in the mouse retina. Invest Ophthalmol Vis Sci 1978;17(6):489–498. [PubMed: 659071]
19. La Vail MM. Survival of some photoreceptor cells in albino rats following long-term exposure to continuous light. Invest Ophthalmol Vis Sci 1976;15(1):64–70.
20. Yu X, Wadghiri YZ, Sanes DH, Turnbull DH. In vivo auditory brain mapping in mice with Mn-enhanced MRI. Nat Neurosci 2005;8(7):961–968. [PubMed: 15924136]
21. Silva AC, Lee JH, Aoki I, Koretsky AP. Manganese-enhanced magnetic resonance imaging (MEMRI): methodological and practical considerations. NMR Biomed 2004;17(8):532–543. [PubMed: 15617052]
22. Calkins D, Horner PJ, Roberts R, Gradianu M, Berkowitz BA. Manganese-enhanced MRI of the DBA/2J mouse model of hereditary glaucoma. Invest Ophthalmol Vis Sci 2008;49(11):5083–5088. [PubMed: 18552381]
23. Pu M, Xu L, Zhang H. Visual response properties of retinal ganglion cells in the Royal College of Surgeons dystrophic rat. Invest Ophthalmol Vis Sci 2006;47(8):3579–3585. [PubMed: 16877432]
24. Kalloniatis M, Tomisich G, Wellard JW, Foster LE. Mapping photoreceptor and postreceptoral labelling patterns using a channel permeable probe (agmatine) during development in the normal and RCS rat retina. Vis Neurosci 2002;19(1):61–70. [PubMed: 12180860]
25. Doyle SE, Castrucci AM, McCall M, Provencio I, Menaker M. Non-visual light responses in the Rpe65 knockout mouse: rod loss restores sensitivity to the melanopsin system. Proc Natl Acad Sci USA 2006;103(27):10432–10437. [PubMed: 16788070]
26. Ohguro H, Ohguro I, Mamiya K, Maeda T, Nakazawa M. Prolonged survival of the phosphorylated form of rhodopsin during dark adaptation of Royal College Surgeons rat. FEBS Lett 2003;551(13): 128–132. [PubMed: 12965217]

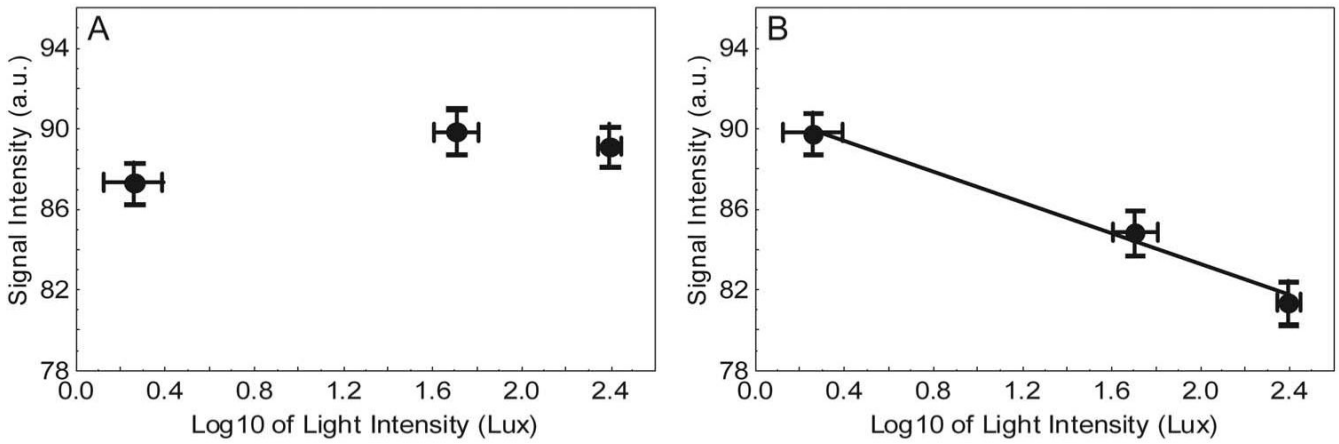

Figure 1.

Summary of changes in MEMRI signal intensity in rats as a function of light intensity in the (**A**) inner and (**B**) outer retina. Error bars, SEM. The *drawn line* is the linear regression line, which was significant only for outer retina (**B**). Since such a relationship was not found for inner retina, no line is shown in (**A**).

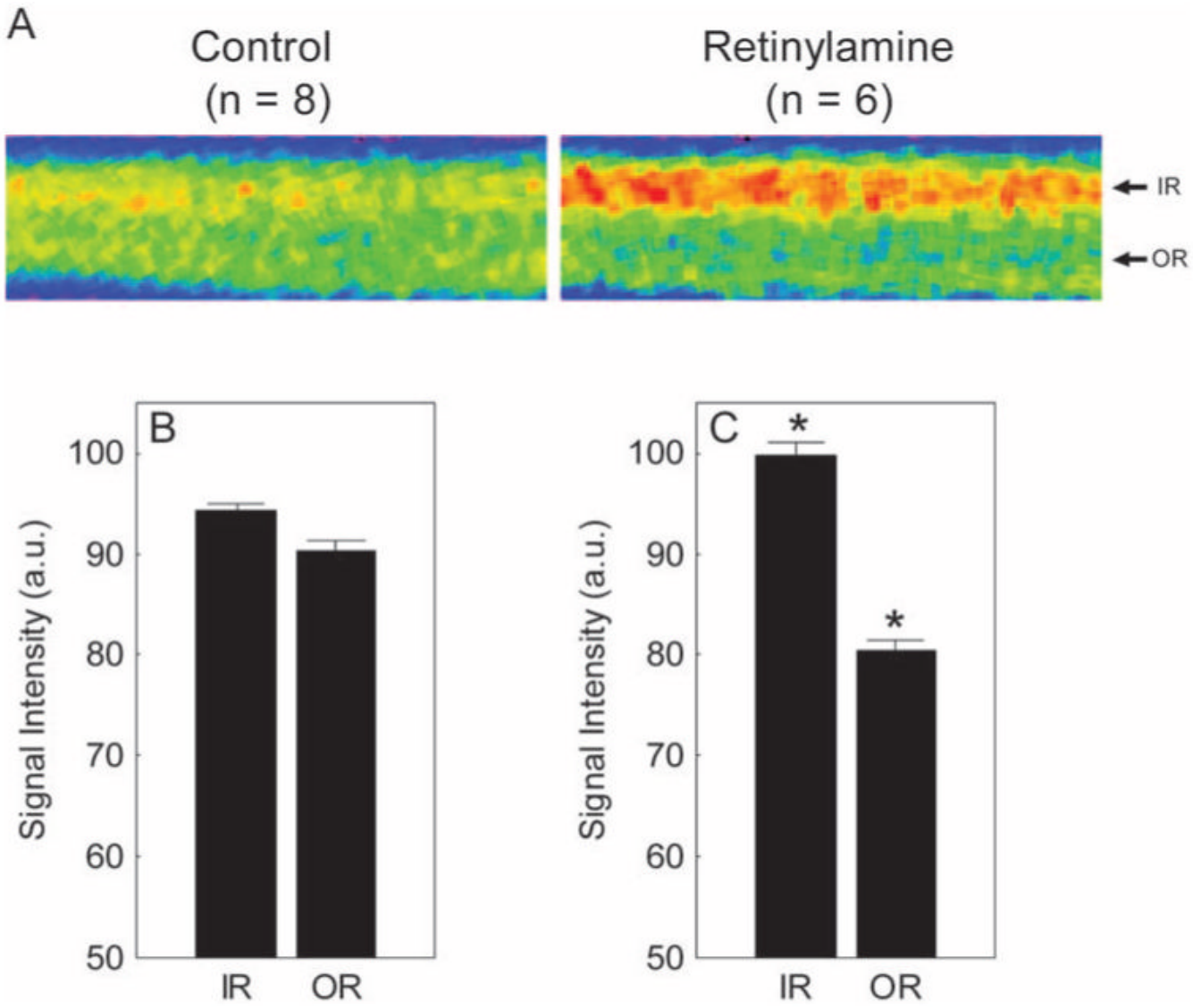

Figure 2.

Summary of changes in MEMRI intraretinal signal intensity due to retinylamine treatment. (**A**) Pseudocolor linearized images of average retinal signal intensity in central retina of dark-adapted control male mice (*left*, control; $n = 8$) and retinylamine-treated mice (*right*, retinylamine; $n = 6$). The same pseudocolor scale was used for both linearized images, where *blue* to *green* to *yellow* to *red* represents the lowest to highest signal intensities. The intraretinal location used to extract the inner retinal (IR) and outer retinal (OR) data are indicated on the *right* of each linearized image. (**B**, **C**) Summary of inner and outer retinal signal intensities for control and retinylamine-treated mice. *Between-group comparisons between respective retinal regions with $P < 0.05$. Error bars, SEM. The *y*-axis scale starts at 50 because this is the premanganese baseline level determined from noninjected mice (data not shown).

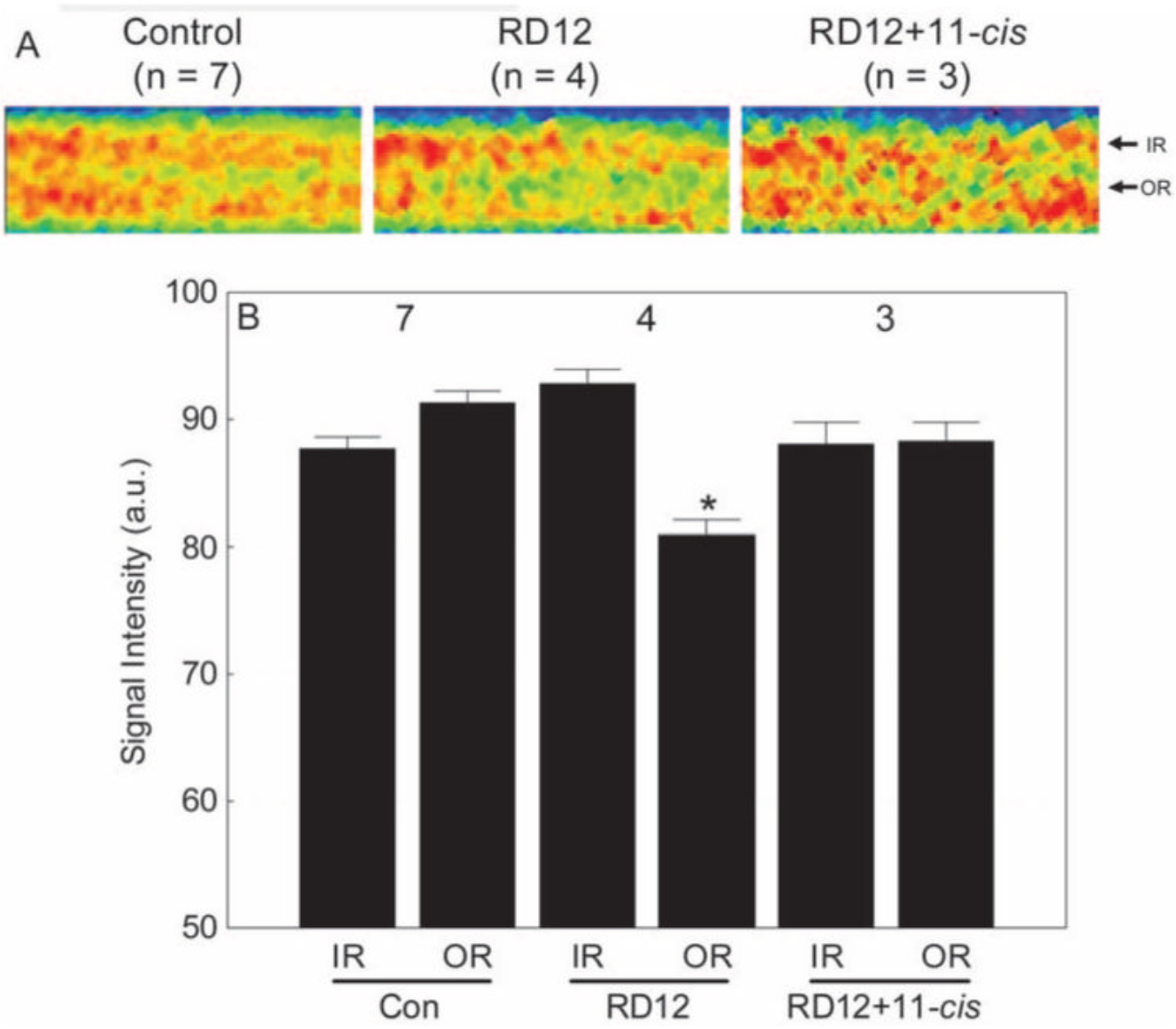

Figure 3.

Summary of inner and outer retinal signal intensities for control, untreated RPE65^{RD12} (RD12), and 11-*cis* retinal-treated RPE65^{rd12} (RD12+11-*cis*) mice. (**A**) For visualization purposes only, pseudocolor linearized images are presented of average retinal signal intensity in central retina of these groups (after setting each groups' inner retinal value to a constant value; based on the quantitative data in **B**). The same pseudocolor scale was used for all linearized images, where *blue* to *green* to *yellow* to *red* represents the lowest to highest signal intensities. (Note the contrast is different from that in Figure 2.) The intraretinal location used to extract inner retinal (IR) and outer retinal (OR) data are indicated on the *right* of each linearized image. (**B**) A quantitative summary of these groups. Comparison to WT control outer retinal signal intensity with $P < 0.05$. Error bars, SEM. The *y*-axis scale starts at 50, the premanganese baseline level determined from noninjected mice (data not shown).